Saunders et al., https://doi.org/10.1083/jcb.201507113

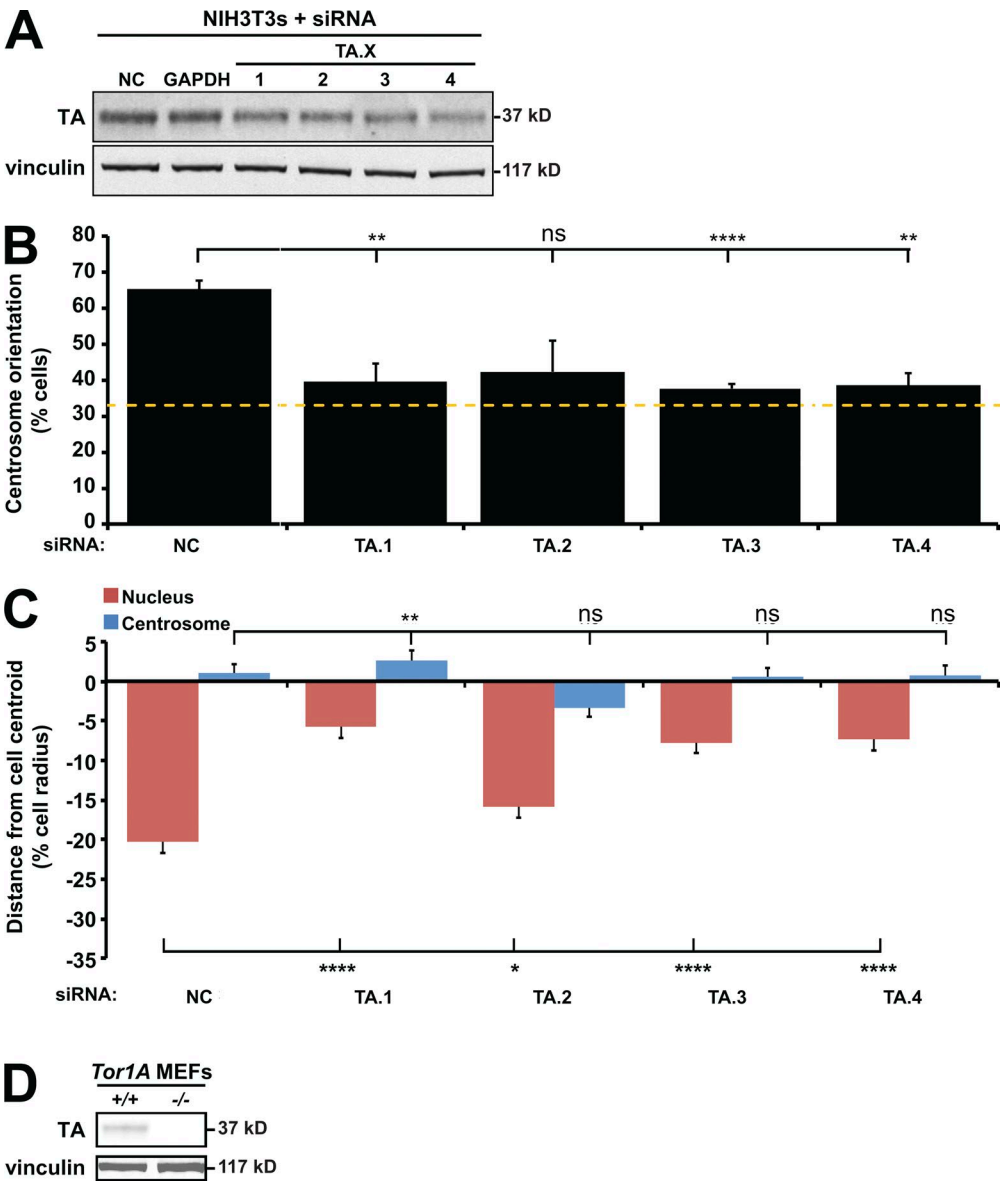

Figure S1. **Validation of torsin protein depletion from NIH3T3 fibroblasts by various siRNAs.** (A) Representative Western blots of lysates from cells treated with siRNA and probed with the indicated antibodies. (B) Centrosome orientation in wound-edge cells treated with the indicated siRNAs. The dashed yellow line denotes random centrosome orientation. (C) Mean centrosome and nucleus positions measured from the cells described in B. $n \geq 183$. (D) Representative Western blots of lysates from *Tor1A*$^{+/+}$ and *Tor1A*$^{-/-}$ MEFs probed with the indicated antibodies. Error bars indicate SEM. *, $P < 0.05$; **, $P < 0.01$; ****, $P < 0.0001$; ns, not significant.

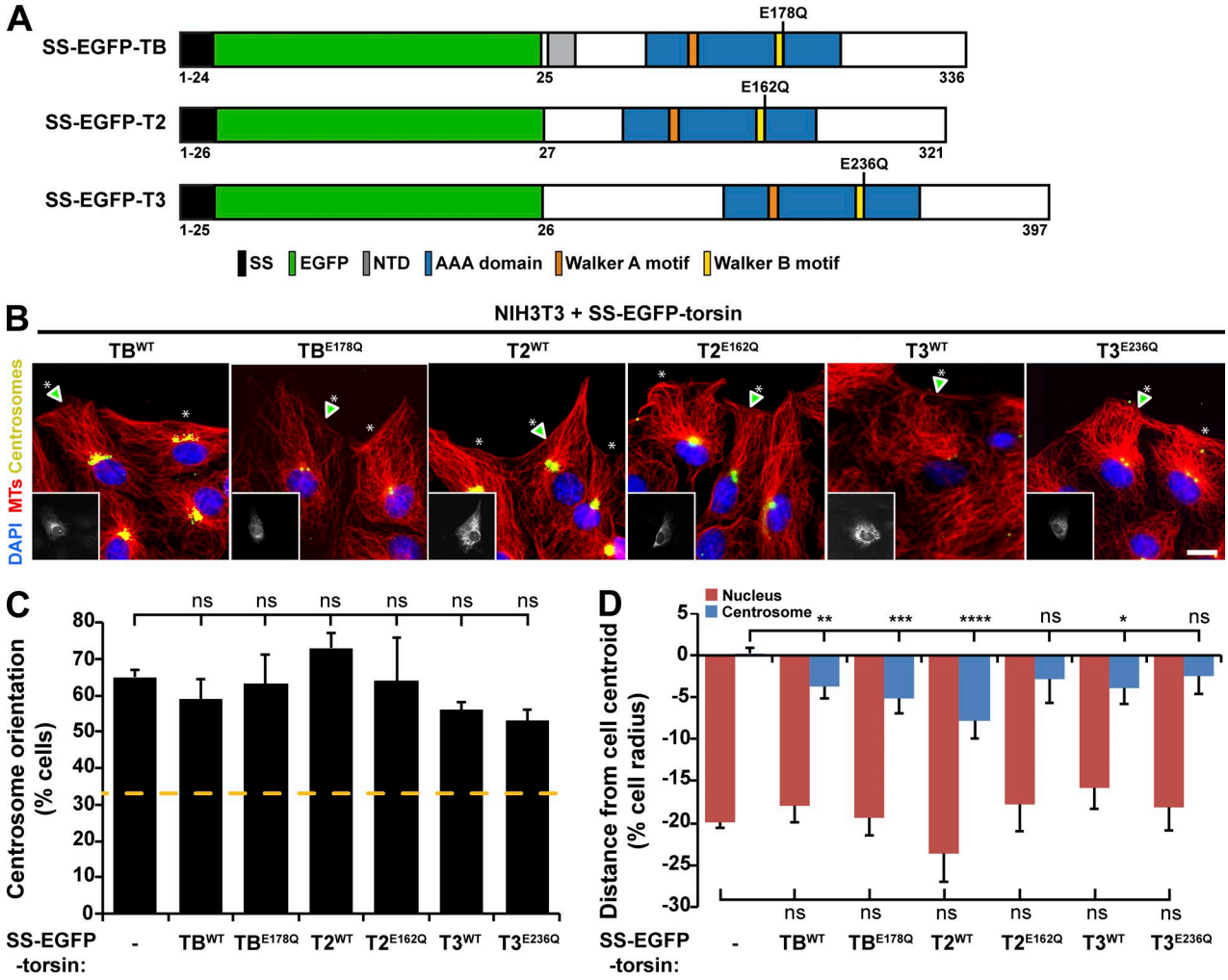

Figure S2. **Testing the roles of TB, T2, and T3 during rearward nuclear positioning and centrosome orientation in NIH3T3 fibroblasts.** (A) Diagram of the SS-EGFP-TB, -T2, and -T3 constructs used in this figure. Protein domains were identified using the SMART platform (Schultz et al., 1998). (B) Representative epifluorescence images of centrosome orientation in cells expressing the indicated SS-EGFP-torsin construct (arrowheads and insets). Asterisks indicate oriented centrosomes. Bar, 10 µm. (C) Centrosome orientation in the cells described in B. The dashed yellow line denotes random centrosome orientation. (D) Mean centrosome and nucleus positions measured from the cells described in B. $n \geq 71$. Error bars indicate SEM. *, $P < 0.05$; **, $P < 0.01$; ***, $P < 0.001$; ****, $P < 0.0001$; ns, not significant.

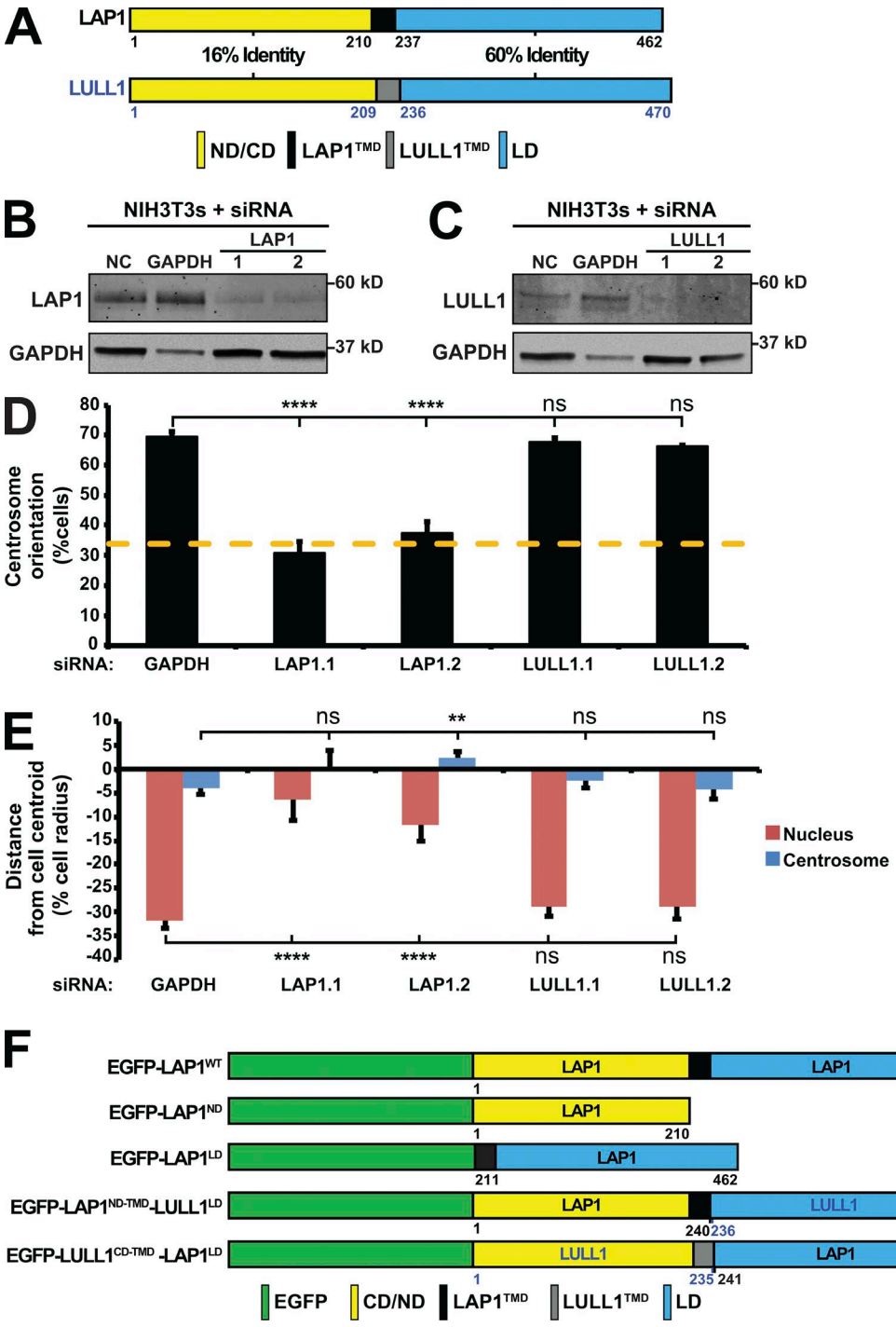

Figure S3. **Validation of LAP1 and LULL1 depletion from NIH3T3 fibroblasts by various siRNAs.** (A) Diagrams of the human LAP1 and LULL1 proteins. (B and C) Representative Western blots of lysates from cells treated with the indicated siRNAs and probed with the indicated antibodies. (D) Centrosome orientation in cells treated with the indicated siRNAs. The dashed yellow line denotes random centrosome orientation. (E) Mean centrosome and nucleus positions from the cells described in D. $n \geq 100$. (F) Diagrams of the EGFP-LAP1 constructs and EGFP-tagged LAP1/LULL1 chimeric constructs used in Fig. 3 (H and I). Error bars indicate SEM. **, $P < 0.01$; ****, $P < 0.0001$; ns, not significant.

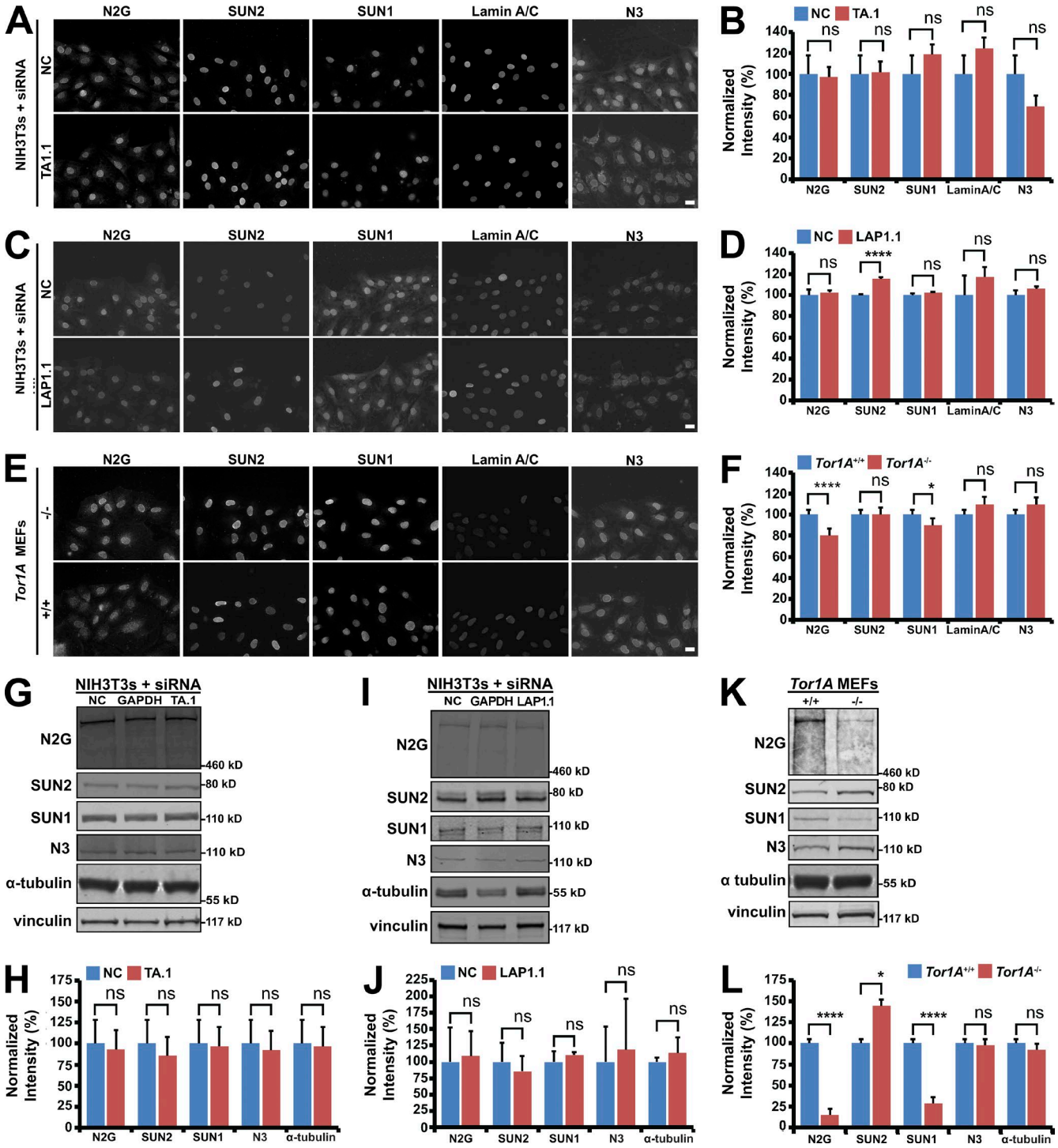

Figure S4. **Quantification of the nuclear and biochemical levels of TAN line components in TA- and LAP1-depleted NIH3T3 fibroblasts as *Tor1A*$^{-/-}$ MEFs.** (A, C, and E) Representative epifluorescence images of cells treated with siRNA and stained with the indicated antibodies. Bars, 20 µm. (B, D and F) Quantification of the nuclear envelope protein levels from the cells described in A, C, and E, respectively. $n \geq 3$. (G, I, and K) Representative Western blots of lysates from the indicated cells probed with the indicated antibodies. (H, I, and L) Quantification of protein levels from the experiments described in G, J, and K, respectively. Error bars indicate SEM. *, $P < 0.05$; ****, $P < 0.0001$; ns, not significant. N3, nesprin-3.

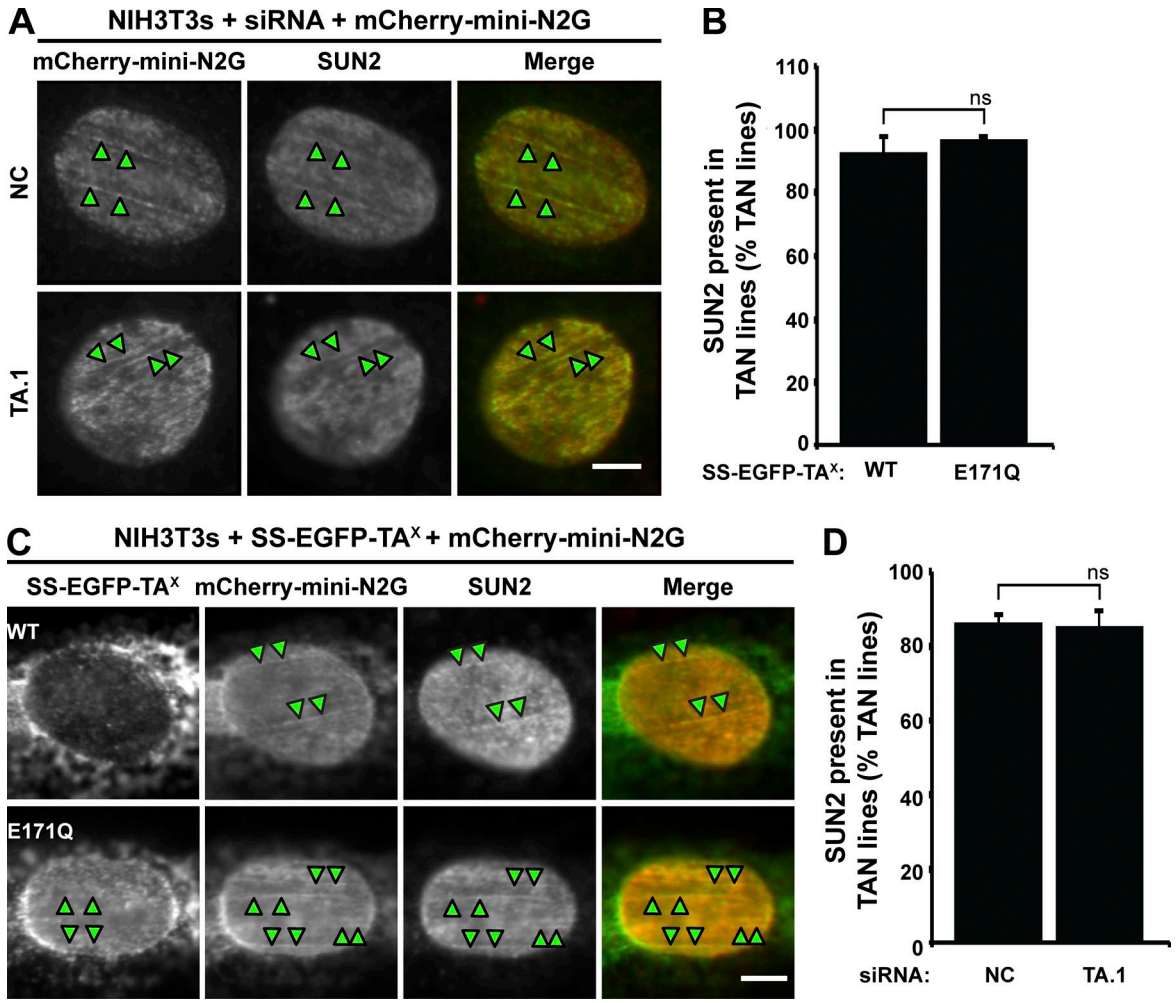

Figure S5. **Quantification of endogenous SUN2 recruitment to TAN lines in NIH3T3 fibroblasts with impaired TA function.** (A) Representative epifluorescence images of cells treated with the indicated siRNAs and expressing mCherry–mini-N2G. (B) Quantification of the percentages of TAN lines with SUN2 recruitment from the cells described in A. $n \geq 81$. (C) Representative epifluorescence images of cells expressing mCherry–mini-N2G along with the indicated SS-EGFP-TA^X construct, as well as representative epifluorescence images of cells treated with the indicated siRNAs and expressing mCherry–mini-N2G. Bars, 5 µm. (A and C) Arrowheads indicate colocalization. (D) Quantification of the percentages of TAN lines with SUN2 recruitment from the cells described in C. $n \geq 84$. Error bars indicate SEM. ns, not significant.

Table S1. **Primers used to generate the constructs used in this paper**

Primer name	Sequence (5′–3′)	RE cut site
TA^{C280S}-F	CACCTAAAAATGAGTATCCGAG	-
TA^{C280S}-R	CTCGGATACTCATTTTTAGGTG	-
TA^{C319S}-F	CAGATAAAGGCAGCAAAACGGT	-
TA^{C319S}-R	CACCGTTTTGCTGCCTTTATCTG	-
EGFP-LAP1^{WT}-F	GG**GGTACC**ATGAAGACGCGAAGGACTAC	KpnI
EGFP-LAP1^{WT}-R	GG**GGTACC**ATGAAGACGCGAAGGACTAC	KpnI
LAP1^{R442A}-F	CCTCTGGAGCGCGATATCTCACTTAGTTCTG	-
LAP1^{R442A}-R	CCATTCAGTTTGTCTGGG	-
LAP1$^{ND\text{-}TMD}$-F	AGTCAG**AAGCTT**GGATGAAGACGCGAAGGACTACC	HindIII
LAP1$^{ND\text{-}TMD}$-R	GCTGGGCTGGAGAGGAATAGTAGCTATTAGTACTAAAGAACCAAAAACTCCCAG	-
LULL1^{LD}-R	CTGACT**GGATCC**TTGAAAAGGCACCCCTGTTC	BamHI
LULL1$^{CD\text{-}TMD}$-F	AGTCAG**AAGCTT**GGATGGCCGACAGTGGACTTAG	HindIII
LULL1$^{CD\text{-}TMD}$-R	CAGCAGTGGTTTCTACCTCAGGCACAGAACTTGCCACAACAGC	-
LAP1^{LD}-R	CTGACT**GGTACC**TTGCAGATGCCCCTTTTCAGGGC	BamHI

F, forward; R, reverse; RE, restriction enzyme (denoted by bold sequences).

Table S2. **Sequences of siRNA duplexes used in this paper**

Gene	siRNA	siRNA sequence (5′–3′)
Gapdh	GAPDH	AAAGUUGUCAUGGAUGACCTT
Tor1aip1	LAP1-1	CAACCUUGAUCUUCUAUATT
	LAP1-2	GGUCAAUUUCUUCGAAGAATT
Tor1aip2	LULL1-1	CGUGAACUCUGAAAGUAAATT
	LULL1-2	GAUGUCUAUUGGUAGUUAATT
NC	NC	UUCUCCGAACGUGUCACGUTT
Syne2	N2G-1	CCAUCAUCCUGCACUUUCATT
Tor1A	TA-1	GAUGCAACAUGGACCUGAATT
	TA-2	GCAAGAUCAUCGCGGAGAATT
	TA-3	CGCCGUGUCUGGUUUCCUATT
	TA-4	GGAACCUCAUAGAUUAUUUTT

The reverse sequence is not depicted.

Reference

Schultz, J., F. Milpetz, P. Bork, and C.P. Ponting. 1998. SMART, a simple modular architecture research tool: identification of signaling domains. *Proc. Natl. Acad. Sci. USA.* 95:5857–5864. http://dx.doi.org/10.1073/pnas.95.11.5857